Journal Name

COMMUNICATION

Protein Nanowires with conductive properties

Anders Elfwing, Fredrik G. Bäcklund, Chiara Musumeci, Olle Inganäs and Niclas Solin

Herein we report on the investigation of self-assembled protein nanofibrils functionalized with metallic organic compounds. We have characterized the electronic behaviour of individual nanowires using conductive atomic force microscopy. In order to follow the self assembly process we have incorporated fluorescent molecules into the protein and used the energy transfer between the internalized dye and the metallic coating to probe the binding of the polyelectrolyte to the fibril.

Interfacing biological systems with electronic conductors is one of the goals of bioelectronics, where recording from biological systems as well as of stimulation of biological processes is desired.[1] The most commonly used conductors are based on elemental metals or semiconductors which are hard materials. In contrast, biological tissue or cells are examples of soft matter. Bioelectronics based on traditional hard electronic conductors thus requires the creation of a hard-soft interface.[2] This hard-soft transition is associated with many problems, including that of mechanical damage. In addition, the hard foreign material may provoke biological defense reactions as the cells have an intrinsic preference for the mechanical properties of their surrounding soft material.[3] For neural interfaces, these are severe problems and much efforts has gone into making materials and structures for the transition from hard to soft materials.[4,5,6] Using the biopolymers found in biological tissue as a geometrical and mechanical scaffold for functionalization with organic polymeric conductors is one way to create materials likely to be tolerated by biological tissue.

Functionalization of biomolecular materials, by methods such as incorporation of fluorescent molecules[7], attachment of plasmonic noble metal particles[8] or in-situ polymerization of functional polymers[9] has been extensively investigated. One attractive category of biomolecular structural scaffolds is amyloid-like protein fibrils. Many proteins share an ability to self-assemble into these mechanically strong and well-ordered fibrous structures.[10] The formation of amyloid fibrils has been intensively studied due to the association of amyloid structures with various diseases such as Alzheimer's disease.[11] It has, however, recently become clear that amyloid fibrils can also have benign and critical functionalities in vivo.[12] From a preparative aspect, an attractive feature of these materials is that they can readily be formed in vitro from various proteins not associated with neurodegenerative diseases. A prominent example is the self-assembly of bovine insulin into amyloid-like fibrils. The preparation of such fibrils is remarkably facile and involves simply dissolving the protein in acidic water followed by heat treatment. The amyloid-like fibrils thus formed have diameters in the nm-range with lengths up to several μm.[13,14] The high level of structural order, generic fibril structure and ease of formation makes amyloid-like fibrils formed in vitro an attractive template for organization of numerous compounds having attractive interactions with the fibrils. The outstanding mechanical and structural properties of protein fibrils have been utilized in a wide variety of applications ranging from bionanocomposites[15], and nano-scaffolds for biosensors[16] to substrates for human cell growth[17].

Conducting polymers, especially poly(3,4-ethylenedioxythiophene) – commonly abbreviated as PEDOT –

have found extensive use in solar cells, OLEDs and electrochemical devices. The excellent electrochemical stability, ease of use and biocompatibility[18,19] have made PEDOT the workhorse of organic electronics. Since PEDOT is highly insoluble and the commercial variant comes as a dispersion in water together with poly(styrene sulfonate) as a dopant, it is, however, not suitable as a functionalization agent for biopolymers. On the other hand, the alkoxysulfonate version of PEDOT, PEDOT-S (Figure 1a) is a fully self doped and water soluble polymer with an intrinsic conductivity of 30 S/cm.[20] PEDOT-S has previously been used in self-assembly processes with silk fibers[21], peptides[22] and DNA[23]. Functionalized amyloid fibrils have been reported by Hamedi *et al* where protein structures were combined with a conducting polymer, thus creating conducting fibrillar networks, which also could be used as an active material in electrochemical transistors.[24] One reason for the rapid interaction between PEDOT-S and larger biomolecular scaffolds is the relative small size of the molecule; PEDOT-S is actually more of an oligomer with a maximum molecular weight around 5500 Da which corresponds to some 16 monomers in length as measured by GPC.[25] This was further supported by MALDI-TOF experiments where PEDOT-S was dropcast onto the MALDI-TOF plate together with dihydroxybenzene as matrix. The resulting mass-spectrum is shown in the ESI (See ESI, Figure S1) where the peaks corresponding to molecular masses of PEDOT-S oligomers of different molecular weight, ranging from 3-mers up to 16-mers are readily observable. Another reason for the strong interaction with other charged molecules is the sulfonate sidegroups. 30 % of the sulfonate groups acts as self-dopants of the conjugated backbone[25], which leaves some of the sulfonate groups to be exploited in electrostatic interactions with positively charged species.

a   b
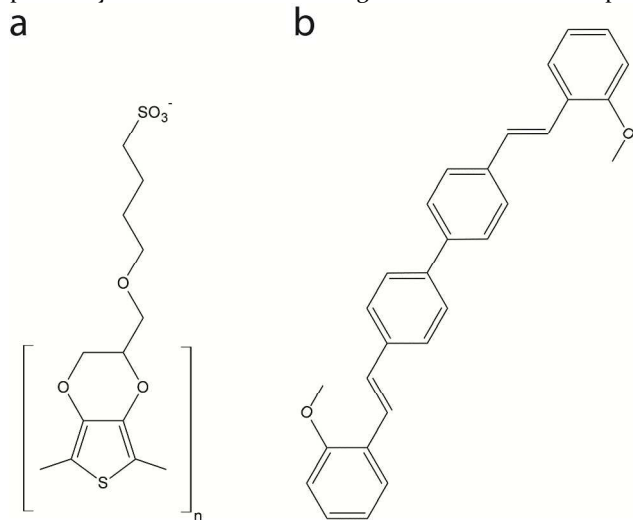
Figure 1 a) The metallic polymer alkoxysulfonated poly(ethylenedioxythiophene) PEDOT-S b) the fluorescent dye molecule 4,4'Bis (2-methoxystyryl)-biphenyl (BMSBP).

In this report we are revisiting the possibility of creating conducting protein nanowires by adding a coating layer of metallic polymer onto a normally insulating protein nanofibril.

In recent years the appearance of various scanning probe microscopy techniques and in particular electrical modes such as conductive atomic force microscopy (C-AFM), have been developed as powerful tools to investigate electronic properties of mesoscopic structures. Examples include a broad range of materials ranging from inorganic nanowires[31] to conducting protein wires[32]. The methodology has also been instrumental in dissecting the electronic properties of DNA[33]. Here we made use of this cutting edge methodology to directly correlate the amyloid fibril morphology and their electric behavior. AFM and C-AFM measurements were carried out in air using a Dimension 3100/NanoScope IV system equipped with a C-AFM module (Veeco, 1 nA/V sensitivity). Commercial silicon cantilevers with a nominal spring constant of 40 N/m were used for morphological characterization in tapping mode and Pt/Ir coated silicon probes with a nominal spring constant of 0.2 N/m were used for electrical characterization in contact mode at constant load force of 5 nN. The fibrils were deposited on glass slides, previously cleaned in an oxidizing solution (5:1:1 MilliQ-water: H_2O_2: 25% NH_4OH). The oxidizing cleaning process creates a negatively charged glass surface to which non-coated amyloid fibrils spontaneously adhered due to favourable electrostatic interactions between the positively charged protein fibrils and the negatively charged glass surface. In fact, rinsing with MilliQ water would not remove significant amounts of fibrils once adhered. The attachment of PEDOT-S coated fibrils to glass proved far more challenging, as the PEDOT-S coated amyloid fibrils adhere poorly to negatively charged surfaces. This phenomena can be explained by the presence of negatively charged PEDOT-S on the protein fibril surface. To enable surface adhesion, clean glass slides were treated with (3-aminopropyl)triethoxysilane (APTES) according to the procedure by Vahlberg *et al* in order to create a positively charged surface.[34] PEDOT-S coated fibrils adhered very strongly to the modified surface and could withstand rinsing with water. We utilized the methodology based on APTES-modified surfaces for various further studies of PEDOT-S coated fibrils. For the electrical characterization by C-AFM the fibrils were drop-cast onto APTES-functionalized glass substrates having patterned ITO electrodes and the conductivity of the fibrils was probed by C-AFM operating in a horizontal configuration.[35] In this setup, a constant voltage is applied to the ITO electrode and current can flow through the organic layer, from the biased lateral contact to the movable metal-coated C-AFM tip. Initial studies of the conductivity of the coated fibrils revealed that we were unable to measure any conductivity of the fibrils by C-AFM even though macroscopic measurements had shown conductivity when using electrode gaps over 25 μm. It was likely that in these cases, the current was carried by a thin film of unbound PEDOT-S and not by the PEDOT-S coated fibrils. At this stage of the process, it was clear that unassociated PEDOT-S had to be carefully removed. Furthermore, an estimation of the amount of PEDOT-S needed to get a sufficient coating of conducting material onto the insulating fibril was called for. To address the latter issue we decided to investigate the PEDOT-S:fibril complexation in more detail. Investigating PEDOT-S:fibril formation is, however, inherently difficult as PEDOT-S does not, unlike other polytiophenes[28], change its optical characteristics upon binding to amyloid like fibrils,. Statistical analysis of fiber morphology, as measured by AFM, is also unreliable.

Bäcklund *et al* has previously reported amyloid like fibrils functionalized with a wide variety of organic fluorescent

molecules located in the fibril interior.[26,27] The fibrillation process leads to a dispersion of the fluorescent molecules within the amyloid framework, thereby increasing the quantum yield of the dye significantly. If we could exploit the non-radiative energy transfer between the internalized molecule and the conducting polymer we could characterize polymer binding to the protein fibril. In order to facilitate such energy transfer experiments it is important to consider the broad absorption spectrum of PEDOT-S (Figure S2). The dye to be incorporated into fibrils was therefore carefully chosen as to have an emission maximum where doped PEDOT-S has an absorption minimum. In order to prepare the protein-dye composite 0.5 mg of the dye 4,4'Bis (2-methoxystyryl)-biphenyl (hereafter named BMSBP), see the structure in Figure 1b) was ground together with 25 mg native bovine insulin (Mw 5733 g/mol, Sigma-Aldrich) according to a previously developed procedure.[27] Fibrils were formed by dissolving the resulting composite material in 5 mL 25 mM hydrochloric acid followed by heating at 65° C for 24h. The resulting material was characterized by UV-vis and fluorescence spectroscopy (See Figure S3 for spectra). The as prepared dispersion of fibrils was diluted in 25 mM HCl to a final concentration of 10 mg/L. PEDOT-S ranging from 0.01 mg/L to 50 mg/L final concentration was subsequently added and the emission spectra (samples excited at 405 nm) were then recorded at various concentrations in a Tecan plate reader. The resulting spectra are shown in Figure 2a and it is clear that an increasing of the PEDOT-S concentration leads to a decrease of BMSBP emission. As the amyloid-like fibrils have diameters of below 10 nm the maximum distance between an internalized dye molecule and the surface would be well within the range of Förster resonance energy transfer which would explain the decrease of BMSBP emission. To verify the existence of quenching we plotted the emission at 440 nm vs the ratio of added PEDOT-S to BMSBP fibrils (w/w) on a linear scale (Figure S4). The decrease in fluorescence follows a quasi-exponential decay and since any absorbance effects on the fluorescent signal would be linear we conclude that BMSBP fluorescence is in fact quenched by the metallic polymer PEDOT-S. When plotting the emission at 440 nm as a function of the PEDOT-S vs. protein ratio on a logarithmic scale (Figure 2b) it follows a sigmoidal shape typical of a saturation process. From these observations we conclude that PEDOT-S is quenching the BMSBP emission and that a ratio of 1:1 (w:w) PEDOT-S to protein is sufficient to achieve maximum quenching of emission of the embedded dye, likely by establishing a quasi-monolayer.

The quenching effect is also readily observed by fluorescence microscopy. Solid films of BMSBP-functionalized uncoated fibrils, deposited on glass by drop casting, are fluorescent (Figure S5a). However, films formed from PEDOT-S coated fibrils show strong quenching of BMSBP emission (Figure S5b).
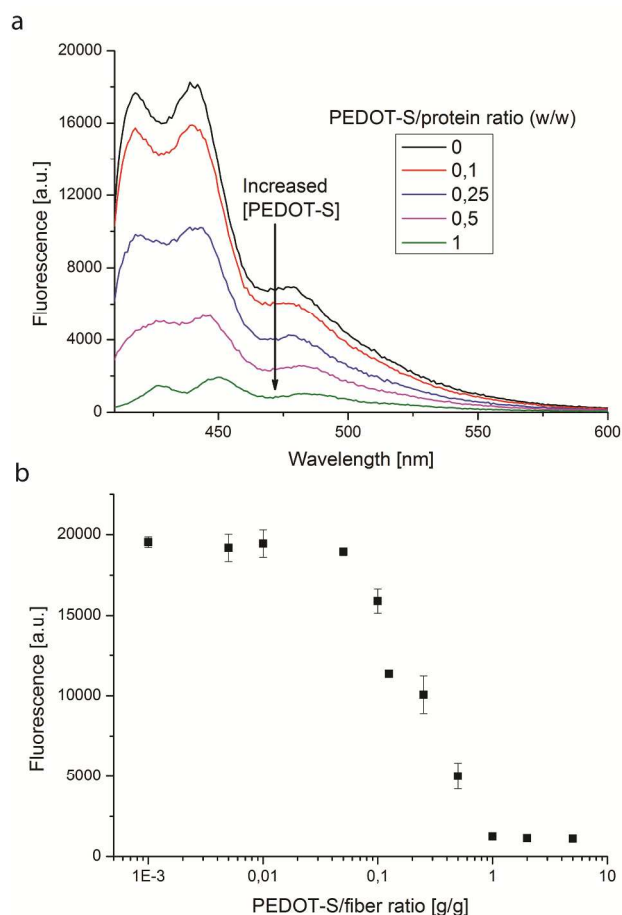
Figure 2 a) Emission spectrum of BMSBP fibrils (0.01 g/L) with added PEDOT-S, the arrow indicates the trend of decrease in emission with increased PEDOT-S concentration. e) The emission at 440 nm plotted as a function of the PEDOT-S vs. protein ratio (w/w) on a logarithmic scale.

The supramolecular interaction between amyloid like fibrils and conjugated polyelectrolytes have been suggested to involve several types of forces such as electrostatic interaction, π-stacking, and hydrophobic interactions.[28,29] Electrostatic interactions may play a major role since at the pH used (pH 2) the protein fibrils are positively charged (the isoelectric point of native insulin being pH 5.3)[30] and the sulfonate groups of the conjugated polymer are negatively charged). To analyze the importance of electrostatic interactions the effect of an increase in salt concentration on PEDOT-S binding was investigated. The BMSBP emission of BMSBP – PEDOT-S fibrils was studied at different salt concentrations. Since high salt concentration would increase screening of charges, the influence of electrostatic forces would consequently decrease. The emission of 10 mg/L BMSBP fibrils with and without 0.5 M NaCl was recorded before and after PEDOT-S addition. PEDOT-S was added to reach a final concentration of 1 mg/L (1:10 polymer to protein weight per weight ratio). The emission at 460 nm was measured when excited at 405 nm using a FLUOstar Galaxy, (BMG Labtechnologies) plate reader. The resulting quenching efficiency in non-salt and salt samples gave 69±7 % and 43±2 % quenching respectively. The decrease in quenching efficiency with increased salt concentration confirmed the importance of electrostatic interactions in PEDOT-S:fibrils complexes. It was,

however, not possible to totally counter-act the quenching, suggesting that although electrostatic forces are dominant, other forces could still be influential.

Our C-AFM studies had, as already mentioned, shown that non fibril-bound PEDOT-S was able to form a conductive film. This artefact complicated the C-AFM characterization of the PEDOT-S:fibril complex. To overcome this obstacles a different preparation route was developed. A high ratio (10:1 w:w) of PEDOT-S to fibrils complexation inevitably leads to the formation of large aggregates. This enabled us to readily separate the PEDOT-S bound to fibrils from the excess PEDOT-S by centrifugation. After 5 minutes of centrifugation at 5000 g the pelleted PEDOT-S: fibril complex was stable enough to allow removal of the excess polymer simply by decanting. The aggregate could then be re-dispersed in MilliQ water giving pure PEDOT-S:fibril complexes that were used in further studies. For the electrical characterization the resuspended pellet was drop-cast onto APTES-functionalized glass

substrates having patterned ITO electrodes. The resulting sample was dried in oven at 65°C for a few minutes, briefly rinsed with MilliQ water, and was dried under a stream of nitrogen. Bare amyloid fibrils, without PEDOT-S processed in the same way (but on surfaces not treated with APTES), spread quite homogeneously on the substrate forming a network of relatively well dispersed fibrils visualized by AFM (Figure S6 a,c). In contrast, the PEDOT-S covered fibrils rather form bundles (Figure S6 b,d), leaving large areas of the substrates uncovered. The presence of PEDOT-S coating the fibrils surface is revealed by comparing their average thicknesses to those of bare fibrils. While the average value for the bare fibrils is 3 nm, the presence of PEDOT-S causes an increase and a spreading of the thicknesses to a range of 5-20 nm (Figure S7). The dramatic increase of fibril thickness can be explained by the formation of a multilayer of conducting material around the fibrils, or of bundles of fibrils aggregated to form larger objects.
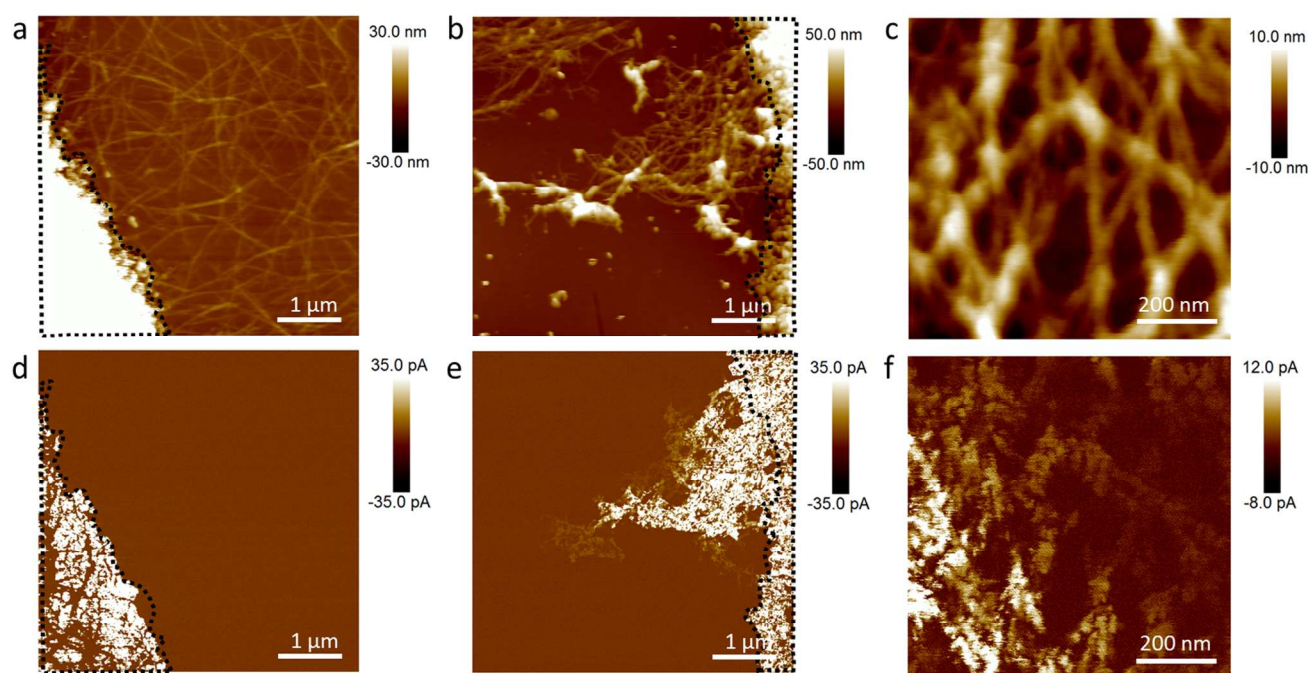
Figure 3. AFM topography images (a-c) and current maps (d-f) of uncovered (a, d) and PEDOT-S covered (b, c, e, f) fibrils. The black dashed lines mark the lateral ITO electrodes. The current maps were obtained by applying to the ITO a voltage of 700 mV (b,d) and 500 mV (f), brighter regions correspond to higher current.

Figure 3 shows AFM images and the relative current maps measured for the bare amyloid fibrils (Figure 3 a,d) and the fibrils covered with PEDOT-S (Figure 3 b,c,e,f). The bare fibrils do not show any conductivity as shown in Figure 3 d. Current is indeed only detected in the region corresponding to the ITO electrode, while the whole surface covered with fibrils show no current signal (brown areas). Consistently, fibril-shaped insulating regions are also visible on top of the ITO electrode (Figure 3d), meaning that even the thin structures act as an efficient barrier for charge injection. Figure 3 b,e show a remarkably different behaviour for the PEDOT-S covered structures. While no current is detected for the fibrils which are not connected to the electrode, a clear conductivity is displayed

for the contacted fibrils. Figure 3 c,f show another sample area at a higher magnification demonstrating the similarity of the fibrillar pattern (Figure 3c) and the corresponding current mapping (Figure 3f).

Currents of tens of pA are obtained at voltages of hundreds of mV with a clear scaling of the current with increasing distance from the lateral electrode, as shown in Figure 4, which is an indication of a lateral charge transport along the fibrils. A higher resolution image, measured in a different area of the sample, is shown in figures 3 e and f. Here the fibrils network is clearly distinguishable and the current features can be easily correlated to the topography image, demonstrating that the

pattern of charge transport corresponds to the pattern formed of PEDOT-S coated fibrils.

Assuming a current of 20 pA at 700 mV bias at a point which is about 5 micrometers away from the electrode (see Figure 4a, segment 1) the effective conductivity of a single nanowire with a diameter of 20 nm would be 10^{-2} S/cm.
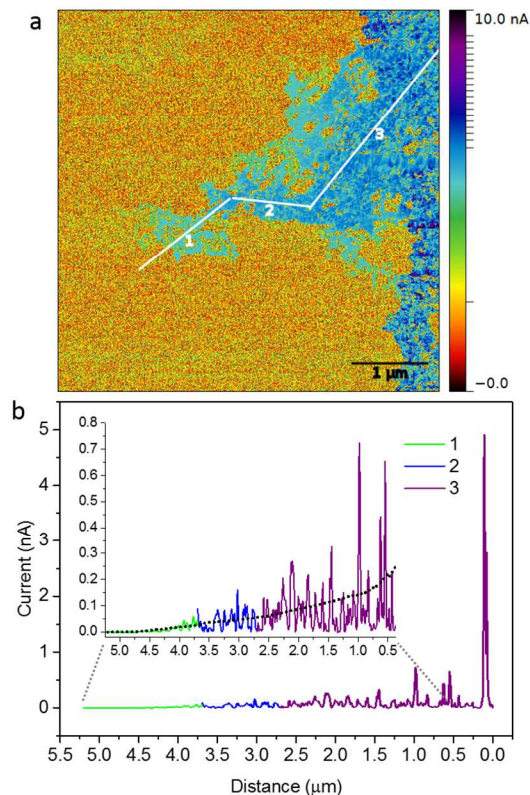
Figure 4. a) Current map (same of Figure 3 d) of PEDOT-S covered fibrils in a non-linear color mapping scale. b) Current profile along the lines marked in a), showing the scaling of the current with the distance from the ITO electrode. The black dotted line in the inset shows the profile trace smoothed through an adjacent averaging method, to guide the eye.

Conclusions

We have created and characterized nanowires based on the self-assembly of insulin amyloid-like fibrils and a conjugated polyelectrolyte. We have used non-radiative energy transfer between a fluorescent molecule and a metallic polymer, where the former is confined on the inside and the latter is attached to the surface of an insulin amyloid-like fibril. With this approach we can study the self-assembly process of fibrils and conjugated polyelectrolytes and have concluded that the electrostatic forces are dominant in the self-assembly process. We have established a new protocol to enhance the self-assembly of conducting material onto the insulating wires, and to remove artefacts, thus enabling us to be able to measure the conductance of individual amyloid fibrils coated with a metallic polymer. This study paves the way for further studies

to create a viable biological interface with appropriate mechanical, structural and electronic properties.

Notes and references

[a] Biomolecular and Organic Electronics, Linköping University, SE-58183 Linköping, Sweden.

Electronic Supplementary Information (ESI) available: S1 MALDI-TOF mass spectrum of PEDOT-S; S2 UV-VIS-Absorption spectrum of PEDOT-S; S3 Excitation/emission spectrum of BMSBP; S4: Fluorescence with and without PEDOT-S; S5 Fluorescence microscopy images of BMSBP fibril films with and without PEDOT-S; S6 AFM images of fibrils with and without PEDOT-S on surfaces; S7 AFM images and histogram describing the thickness of fibrils with and without PEDOT-S. See DOI: 10.1039/c000000x/

1   R. M. Owens and G. G. Malliaras, *MRS Bull.*, 2011, **35**, 449–456.

2   M. Ulbrich and P. Fromherz, *Adv. Mater.*, 2001, **13**, 344–347.

3   D. E. Discher, P. Janmey and Y.-L. Wang, *Science*, 2005, **310**, 1139–43.

4   A. Larmagnac, S. Eggenberger, H. Janossy and J. Vörös, *Sci. Rep.*, 2014, **4**, 7254.

5   M. Asplund, T. Nyberg and O. Inganäs, *Polym. Chem.*, 2010, **1**, 1374.

6   T. Nyberg, O. Inganäs and H. Jerregård, *Biomed. Microdevices*, **4**, 43–52.

7   A. Rizzo, O. Inganäs and N. Solin, *Chem. Eur. J*, 2010, **16**, 4190–5.

8   R. Schreiber, J. Do, E.-M. Roller, T. Zhang, V. J. Schüller, P. C. Nickels, J. Feldmann and T. Liedl, *Nat. Nanotechnol.*, 2014, **9**, 74–8.

9   P. Nickels, W. U. Dittmer, S. Beyer, J. P. Kotthaus and F. C. Simmel, *Nanotechnology*, 2004, **15**, 1524–1529.

10   T. P. J. Knowles and M. J. Buehler, *Nat. Nanotechnol.*, 2011, **6**, 469–79.

11   F. Chiti and C. M. Dobson, *Annu. Rev. Biochem.*, 2006, **75**, 333–66.

12   C. L. L. Pham, A. H. Kwan and M. Sunde, *Essays Biochem.*, 2014, **56**, 207–19.

13   R. Khurana, C. Ionescu-Zanetti, M. Pope, J. Li, L. Nielson, M. Ramírez-Alvarado, L. Regan, A. L. Fink and S. A. Carter, *Biophys. J.*, 2003, **85**, 1135–1144.

14   L. Nielsen, S. Frokjaer, J. F. Carpenter and J. Brange, *J. Pharm. Sci.*, 2001, **90**, 29–37.

15   T. Oppenheim, T. P. J. Knowles, S. P. Lacour and M. E. Welland, *Acta Biomater.*, 2010, **6**, 1337–41.

16   S. M. Pilkington, S. J. Roberts, S. J. Meade and J. A. Gerrard, *Biotechnol. Prog.*, **26**, 93–100.

17   N. P. Reynolds, M. Charnley, R. Mezzenga and P. G. Hartley, *Biomacromolecules*, 2014, **15**, 599–608.

18   S. M. Richardson-Burns, J. L. Hendricks, B. Foster, L. K. Povlich, D.-H. Kim and D. C. Martin, *Biomaterials*, 2007, **28**, 1539–52.

19   M. H. Bolin, K. Svennersten, X. Wang, I. S. Chronakis, A. Richter-Dahlfors, E. W. H. Jager and M. Berggren, *Sensors Actuators B Chem.*, 2009, **142**, 451–456.

20   K. M. Persson, R. Gabrielsson, A. Sawatdee, D. Nilsson, P. Konradsson and M. Berggren, *Langmuir*, 2014, **30**, 6257–66.

21   C. Müller, R. Jansson, A. Elfwing, G. Askarieh, R. Karlsson, M. Hamedi, A. Rising, J. Johansson, O. Inganäs and M. Hedhammar, *J. Mater. Chem.*, 2011, **21**, 2909–2915.

22   M. Hamedi, J. Wigenius, F.-I. Tai, P. Björk and D. Aili, *Nanoscale*, 2010, **2**, 2058–61.

23   M. Hamedi, A. Elfwing, R. Gabrielsson and O. Inganäs, *Small*, 2013, **9**, 363–8.

24   M. Hamedi, A. Herland, R. H. Karlsson and O. Inganäs, *Nano Lett.*, 2008, **8**, 1736–40.

25   K. M. Persson, R. Karlsson, K. Svennersten, S. Löffler, E. W. H. Jager, A. Richter-Dahlfors, P. Konradsson and M. Berggren, *Adv. Mater.*, 2011, **23**, 4403–8.

26   F. G. Bäcklund and N. Solin, *ACS Comb. Sci.*, 2014, **16**, 721–9.

27   F. G. Bäcklund, J. Wigenius, F. Westerlund, O. Inganäs and N. Solin, *J. Mater. Chem. C*, 2014, **2**, 7811.

28   K. P. R. Nilsson, P. Hammarström, F. Ahlgren, A. Herland, E. A. Schnell, M. Lindgren, G. T. Westermark and O. Inganäs, *Chembiochem*, 2006, **7**, 1096–104.

29   A. Herland, D. Thomsson, O. Mirzov, I. G. Scheblykin and O. Inganäs, *J. Mater. Chem.*, 2008, **18**, 126–132.

30   A. Conway-Jacobs and L. M. Lewin, *Anal. Biochem.*, 1971, **43**, 394–400.

31   G. Cheng, S. Wang, K. Cheng, X. Jiang, L. Wang, L. Li, Z. Du and G. Zou, *Appl. Phys. Lett.*, 2008, **92**, 223116.

32   M. Y. El-Naggar, G. Wanger, K. M. Leung, T. D. Yuzvinsky, G. Southam, J. Yang, W. M. Lau, K. H. Nealson and Y. A. Gorby, *Proc. Natl. Acad. Sci. U. S. A.*, 2010, **107**, 18127–31.

33   L. Cai, H. Tabata and T. Kawai, *Nanotechnology*, 2001, **12**, 211–216.

34   C. Vahlberg, G. R. Yazdi, R. M. Petoral, M. Syvajarvi, K. Uvdal, A. L. Spetz, R. Yakimova and V. Khranovsky, in *IEEE Sensors, 2005.*, IEEE, 2005, pp. 504–507.

35   C. Musumeci, A. Liscio, V. Palermo and P. Samorì, *Mater. Today*, 2014, **17**, 504–517.

We have investigated protein fibrils decorated with metallic polymers using conductive AFM
98x40mm (300 x 300 DPI)